12th INTERNATIONAL SCIENTIFIC CONFERENCE ON DEFENSIVE TECHNOLOGIES
OTEH 2026
Serbia, Tara, 21 - 24 October 2026

CFD-BASED NUMERICAL SIMULATION OF THERMAL PROCESSES AND AIRFLOW IN THE PASSENGER COMPARTMENT OF SPECIAL VEHICLE

MILICA IVANOVIĆ
University of Belgrade, Faculty of Mechanical Engineering, Belgrade, Serbia mivanovic@mas.bg.ac.rs

SNEŽANA MALIŠIĆ
Technical Test Center, Belgrade, Serbia, snezana.malisic@toc.urio.vs

MARIJA BALTIĆ
University of Belgrade, Faculty of Mechanical Engineering, Belgrade, Serbia mbaltic@mas.bg.ac.rs

IGOR STAMENKOVIĆ
University of Belgrade, Faculty of Mechanical Engineering, Belgrade, Serbia istamenkovic@mas.bg.ac.rs

Abstract: *Special vehicles frequently encounter numerous challenges to achive and maintain adequate thermal comfort in the passenger compartmen, such as high external temperatures and sun radiation, significant heat generation from onboard equipment and engine, limited space, problems with disposition of supply and exhaust vents, etc. In this paper, a CFD-based numerical simulation of airflow and thermal processes in the passenger compartment of a special vehicle is presented. A three-dimensional model of the enclosed space is developed, which includes internal heat sources from occupants and onboard equipment, as well as external thermal loads introduced via appropriately calculated heat flux boundary conditions. Thermal conditions within enclosed compartments of vehicles for special purpose are governed by complex interactions between airflow, heat transfer and surface radiation. Approach based on CFD can offer detailed insights into airflow dynamics and temperature distribution, which helps address varying thermal comfort levels in enclosed spaces (evaluated using the Predicted Mean Vote (PMV) and Predicted Percentage of Dissatisfied (PPD) indices). Numerical model presented in the paper is validated against experimental data of PPD and PMV values and average cabin temperature. The temperature and velocity distributions obtained through CFD simulation demonstrate the capability of this method to serve as a valuable tool for evaluating thermal comfort, as it enables detailed analysis at any surface, plane or point of interest within the domain. From the other side, CFD introduces the challenge of determining whether a simplified model can simultaneously ensure computational efficiency with reliable predictive capability for the specific HVAC systems in special purpose vehicle, on which some conclusions are given.*

Keywords: *thermal comfort, PMV, PPD, vehicle HVAC system, CFD.*

1. INTRODUCTION

In special-purpose vehicles (such as military, emergency response, security vehicles, etc.) maintaining appropriate thermal conditions presents significantly greater challenges than in conventional passenger cars. These vehicles frequently operate under severe environmental conditions combined with geometric parameters, such as: compact cabin layouts and enhanced structural protection that adds load by means of heat accumulation of the structure (higher thermal mass). Furthermore, high internal heat loads can be generated by electronic equipment along with prolonged mission durations. Occupants frequently wear protective clothing and equipment, which influences heat exchange between the human body and the surrounding environment.

In the commercial automotive sector, the quality of the climate control system is often regarded as an important factor influencing customer satisfaction and vehicle competitiveness. Consequently, considerable effort is devoted to analyzing, optimizing, sizing and validating HVAC systems to achieve high levels of thermal comfort and energy efficiency. The situation is relatively different for special and military vehicles in which operational capability, reliability and crew protection are primary, rather than thermal comfort [1]. As a result, air-conditioning systems have traditionally received less attention during the initial design stages and are frequently incorporated using empirical practices or simplified design procedures. Considering military and urgent systems, already stressful service is enhanced by working in hot environment.

The distribution of temperature, airflow velocity and pressure within an enclosed vehicle compartment is governed by complex fluid flow and heat transfer phenomena. Because of the nature of this interacting mechanisms, predicting the thermal performance of a passenger compartment only through experimental testing

Corresponding author: M. Ivanović;
E-mail: mivanovic@mas.bg.ac.rs
DOI: 10.5937/OTEH26156I

is often time-consuming, expensive and limited to a relatively small number of operating conditions. Under these conditions, conventional methods for HVAC sizing and control are no longer sufficient.

The application of CFD (Computational Fluid Dynamics) analysis in the initial stage of design and afterwards for the evaluation of system work, enables engineers to evaluate multiple design configurations without extensive and expensive experimental testing. Numerical simulations enable investigation of the air temperature influence of supply air diffuser location, airflow, ventilation, radiation and cabin geometry on the resulting thermal and flow field. Additionaly, CFD simulation facilitates the identification of recirculation zones, dead-air regions and temperature non-uniformities that may reduce occupant comfort or impair equipment reliability. Such analyses support engineering decisions during the development and optimization of vehicle HVAC system.

The objective of this paper is to perform a CFD-based numerical simulation of the thermal processes and airflow within the passenger compartment of a special-purpose vehicle, with the aim of validating a simplified geometric and numerical model against experimental data of PMV and PPD value and average cabin temperature. This approach naturally raises the question of the extent to which such a model can be both computationally efficient, cost-effective and accurate.

The investigation focuses on predicting the three-dimensional distributions of air velocity and temperature under representative operating conditions.

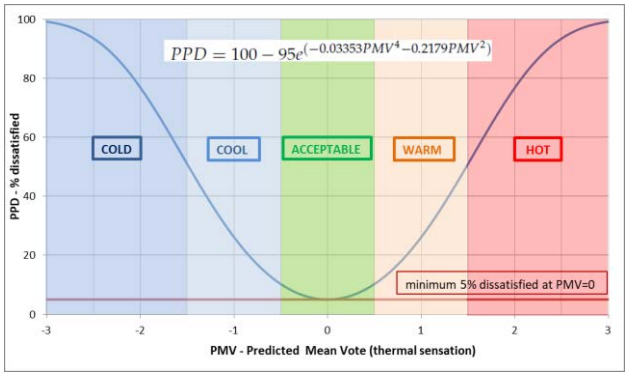
1.1. PPD/PMV indices and standards

Predicted Percentage of Dissatisfied (PPD) is a comfort index that quantifies the expected proportion of occupants dissatisfied with their thermal environment. It is derived directly from the Predicted Mean Vote (PMV) index, which expresses the average thermal sensation of a group on a seven-point thermal sensation scale. This indices are standardized in ISO 7730 standard (Serbian SRPS EN ISO 7730:2008: Ergonomics of the thermal environment - Analytical determination and interpretation of thermal comfort using calculation of the PMV and PPD indices and local thermal comfort criteria. Along with this standard, ANSI/ASHRAE Standard 55: Thermal Environmental Conditions for Human Occupancy, also rely on PMV/PPD model. ASHRAE 55 defines the acceptable comfort zone as a PMV between -0.5 and +0.5 (meaning ≥ 80% of occupants are satisfied), while ISO 7730 splits this into strict categories (A, B, C) where Class B roughly mirrors ASHRAE's requirements. ISO 7730 also includes local discomfort criteria (radiant asymmetry, draft, floor temperature, thermal stratification).

Air speed has a large effect in warm conditions and is explicitly addressed in provisions of ASHRAE 55 standard. Understanding how these parameters interact helps designers create HVAC systems that achieve occupant satisfaction along with energy efficiency. ASHRAE Standard 55 features a highly adopted Adaptive Comfort Model, which sets dynamic indoor temperature targets based on outdoor climates, while ISO 7730 uses a more rigid approach based on the original Fanger PMV formulas.

The curve from Figure 1 shows PMV/PPD functional dependency with highlight that even under ideal thermal conditions (PMV = 0), at least 5% of people remain dissatisfied which is reflection of individual variation in comfort perception. That is why the PPD index ranges from 5% to 100%, with lower values representing higher comfort levels.

Figure 1. PPD — PMV diagram



The variables of importance to evaluate this indices are the function of design and environmental factors throughout a space:

- temperature (uneven thermal distribution increases discomfort),
- air velocity (low or high velocities can lead to stagnation spots or higher local cooling),
- occupant activity and clothing (metabolic rates (met) and clothing insulation (clo) affect PMV and PPD results),
- humidity (direct impact on evaporative cooling and related effects of perceived temperature),
- asymmetry in radiation (localized discomfort with warm and cold surfaces present).

1.2. Vehicle heat load

Sources of the heat that represent vehicle heat load are ambient and radiation load, engine load, metabolic load and exhaust. Loads can be separated based on the placement into two main groups: outer and internal gains. Outer heat gains are:

- direct Sun radiation,
- diffuse radiation (Sun atmospheric scattering),
- conduction load (ambient),
- ground reflected,
- exhaust heat of the vehicle (rejected by the engine and transferred in the vicinity of the cabin).

Internal heat gains are:

- engine heat (rejected by the engine and transferred into the cabin),
- metabolic heat of the occupants,
- onboard electronic equipment radiation.

3. NUMERICAL MODEL

The researched vehicle has an armored, air-conditioned

cabin and it allows the combat team to operate continuously in a hermetically sealed area protected from NBI (Nuclear-Biological-Chemical) threats. HVAC system completely works in air recirculation mode. Geometry of the simplified cabin model is given in Figure 2.

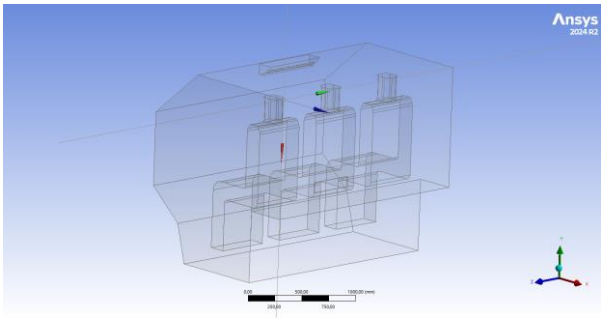


Figure 2. Geometry of the cabin model with occupants

Air circulation in air conditioning mode is carried out through the air distribution system located under the cabin roof and air distribution elements in the front, while exhaust is at the back side of the cabin, which is depicted in Figure 2.

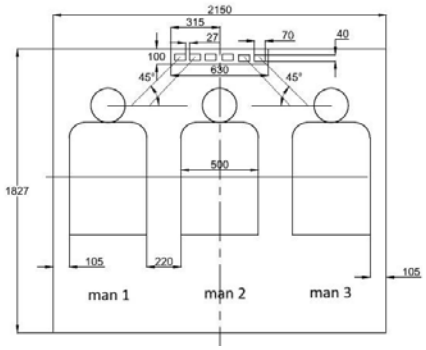


Figure 3. Disposition of supply vents and occupants

Since the simulation of special vehicle that accounts for all potential heat sources is computationally expensive, and moreover, there will be a lot of uncertanty in the final results due to the nature of multiple heat sources, the simplified model has been applied. That model accounts heat gains from the outside (radiation and convection) and electrical equipment radiation, as well as metabolic heat gains, all represented via total heat flux on the particular surfaces (W/m^2).

3.1. Boundary conditions

Experimental condition for air flow is 480 m^3/h, which calculated for the inlet geometry gives v=7,93 m/s. There are six section of the inlet, divided by two for every occupant. The mark of the occupant from the Figure 3 corresponds to the mark of the inlet section. In order to get airflow on every passenger, velocity inlet boundary conditions (BC) are given as components in *x-y-z* direction (Table 2). Turbulence intensity of 5%, and a turbulent-to-laminar viscosity ratio of 10 were set within inlet BC. Inlet temperature is set to 14°C to all sections. Pressure outlet BC was applied at the exit of computational domain. Under this formulation, all flow variables are assumed invariant along the outlet direction, with the exception of the velocity gradient normal to the exhaust plane, while the static pressure at the outlet is set equal to atmospheric pressure.

Table 1. Velocity inlet boundary condition

i	v_x	v_y	v_z
1	$v \cdot \sin(45^\circ) \cdot \cos(45^\circ)$	$-v \cdot \cos(45^\circ)$	$v \cdot \sin(45^\circ) \cdot \sin(45^\circ)$
2	$v \cdot \sin(45^\circ)$	$-v \cdot \cos(45^\circ)$	0
3	$v \cdot \sin(45^\circ) \cdot \cos(45^\circ)$	$-v \cdot \cos(45^\circ)$	$-v \cdot \sin(45^\circ) \cdot \sin(45^\circ)$

Heat flux boundary conditions applied to the vehicle cabin surfaces (except windshield) were determined using the sol-air temperature method (simplifying heat gain calculations by combining ambient air temperature, solar radiation and thermal radiation into a single equivalent outdoor temperature) for all surfaces except windshield. This condition is combined with one-dimensional steady-state conduction through the composite armored and insulatied wall. The daily solar insolation for is Belgrade in July is 6.4 kWh/m²/day (Global horizontal) [2], which converted to peak current flux gives 657 W/m². Considering more conservative approach of "clear-sky" peak values, which other autors used (930 W/m² in [3], 875 W/m² in [4], and 1120 W/m² in [5]), we decided to use I_{solar} = 900 W/m². The absorbed solar flux was calculated using a paint solar absorptivity of α = 0.85, derived from the absorbed-to-incident irradiance ratio reported in [5], which gives absorbed flux on the outer surface of 765 W/m². The external sol-air temperature ($T_{sol-air}$) is calculated using the ASHRAE Handbook heat balance relationship:

$$T_{sol-air} = T_o + \frac{\alpha \cdot I_t}{h_o} - \frac{\varepsilon \cdot \Delta R}{h_o} \quad (1)$$

With a safety margin for summer period the third member is omitted. The external convective heat transfer coefficient was calculated using the correlation from [1], yielding $h_{ext} \approx 29.5$ W/m²K at a vehicle speed of 30 km/h. The sol-air temperature was then used together with the thermal resistance of the 30 mm armor (λ = 15 W/m·K) [6] and 16 mm insulation (λ = 0.035 W/m·K) [7], to determine the interior wall heat flux driven by the difference between the sol-air temperature and the target cabin interior temperature of 26 °C. To account for reduced solar exposure, the effective irradiance on the sides and rear walls was assumed to be around 70% of the roof value.

The total incident solar heat flux on the tilted windshield (at a tilt angle of 40°) was determined by considering direct, diffuse, and reflected radiation components under peak summer conditions in Belgrade at 13:00 h. The direct radiation component was computed by modulating the Direct Normal Irradiation (DNI) with the cosine of the solar angle of incidence (θ), while the Diffuse Horizontal Irradiation (DHI) and Global Horizontal Irradiation (GHI) were scaled using the respective sky and ground view factors, incorporating a standard asphalt albedo of ρ_g = 0.15. To evaluate the actual thermal energy penetrating the cabin through the athermic glass, the calculated total

incident flux was coupled with a standard Solar Heat Gain Coefficient (SHGC=0.40).

Radiative heat transfer from onboard electronic equipment was estimated using the Stefan–Boltzmann relation with an emissivity of 0.9, surrounding temperature of 26 °C, and equipment surface temperatures of 50°C. Heat fluxes generated by the occupants are accounted according to the chosen one for estimating PMV/PPD values during experimental testing. Resulting heat fluxes and surface emissivities implemented as BC are given in the Table 2.

Table 2. Surface heat fluxes and emissivities

Section	Heat flux (W/m^2)	Emissivity
roof	90	0,9
windshield	180	0,9
rear	65	0,9
bottom	30	0,85
front (el.equipment)	150	0,9
sides	65	0,9
man 1	70	0,95
man 2	70	0,95
man 3	70	0,95

3.2. Mesh convergence

Discretization, flow and thermal calculations were performed using ANSYS Fluent [8][8]. A polyhedral mesh was formed with local sizing/refinement in the zones of the ventilation openings and on the occupants. Along the walls of the cabin and around bodies, 4 layers of the boundary layer with a growth factor of 1.2 were formed. The independence of the solution from the mesh density was confirmed with the analysis of three levels of mesh refinement (0.8, 1.2 and 2.2 million cells), where the difference in average cabin temperature was less than 0,3 % between medium and fine mesh (volume averaged temperatures in fluid domain were: 297,84 K, 299,31 K and 300,01K), so medium mesh was adopted for further simulations.

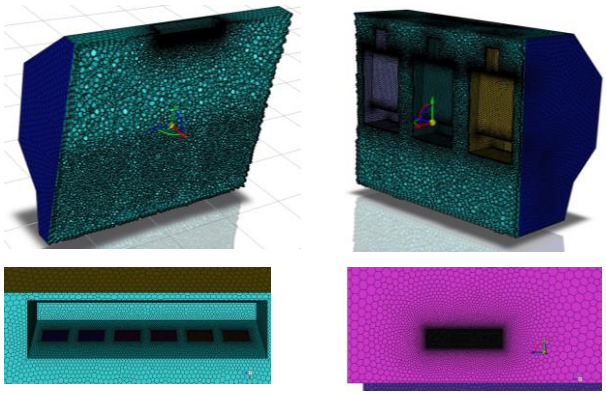


Figure 4. Details of the mesh

3.3. Methods

Radiative heat transfer from the heat sources was modeled using the Discrete Ordinates (DO) radiation model, whereas buoyancy-induced airflow arising only from density gradients within the cabin was accounted with Full buoyancy effects.

Turbulence closure was achieved through a modified two-equation Realizable k-ε model, along with Enhanced Wall Treatment and with Thermal Wall Function.

In the initial phase (first 300 iterations), the pressure-velocity coupling was managed via the SIMPLEC algorithm, combined with First-Order Upwind schemes for the momentum, energy and turbulence equations to establish a stable, non-oscillatory initial flow field. Pressure discretization was done with Body-force-weighted scheme.

For the secondary phase, the solution configuration was advanced to the Coupled algorithm to simultaneously solve the mass and momentum equations. In order to more accurately capture the buoyancy-induced flows driven by significant temperature gradients within the cabin, the pressure discretization was upgraded to the PRESTO! (PREssure STaggering Option) scheme, which is suited for natural convection with higher Rayleigh number. Spatial discretization for the remaining transport variables was elevated to the Second order upwind scheme.

Given the numerical instability inherent in coupled forced and natural convection regimes, the pseudo-transient formulation was included. The Time scale factor was systematically managed, initiating at lower bounds (1e-3) to damp transient numerical fluctuations during the transition to higher order discretization. The residuals stably converged below the thresholds of 1e-3 for continuity and 1e-6 for energy.

4. RESULTS

4.1. Experimental results

Experimenntal testing was conducted after system reached a steady-state thermal condition. Air temperature and velocity, relative humidity (RH), cabin pressure and radiant temperature were measured using sensors for each quantity, over a duration of 5 minutes with a sampling frequency of 1 s. The sensors were positioned at multiple points on different cabin segments (the height at which the sensors are placed is 1,1 m and 0,1 m from the floor of the vehicle as defined in the ISO 7730). This measurement protocol provided a sufficient number of time points (300 samples per sensor).
During the measurement, it was observed that the speed of air flow in the zone around the head is uneven. Unfortunately, technical possibilities and space dictate limitations. Those limitation cannot be changed.
Based on the measured values and using assumed values of metabolic rate, clothing thermal insulation (normal business wear; 0,154 m²K/W clo=0,57) and activity (sitting down, light activity; 70 W/m²; met=1,2), PMV and PPD indices were calculated according to Fanger's thermal comfort model, as defined in the ISO 7730 standard. The air speed was measured in front and was 2 m/s in the narrow zone where it was measured.

The results of average values, as well as extreme values are given in Table 3.

Table 3. Experimental data of temperatures and RH

	t_1, °C	t_2, °C	t_3, °C	%, RH
Average	26,8	25,8	27	36,1
Max.	27	26,1	27,1	39,4
Min.	26,5	25,2	26,6	35,2

Measured values resulted in values of PMV and PPD presented in Table 3.

Table 3. Obtained values of PMV and PPD

	PMV	PPD
Average	0,8	18,5
Maximum	1	22,1
Minimum	0,7	15,3

4.2. CFD results

For the purpose of simplification of the numerical model, relative humidity (RH) was not included in the CFD analysis. Experimental data of this variable showed only 4,2% difference between minimal and maximum value. For the calculation of PMV/PPD values, the average RH was used. Obtained value of average volume in fluid domain are 26,2 °C, while the temperatures at the surface of the passengers are given in Table 4. Surface averaged velocity for the plane created in front of the bodies (at the distance of 10 cm from the chest area) is 0,433 m/s.

Table 4. Numerical results for the body surface of the occupants

	Man 1	Man 2	Man 3
Surface averaged temperature, °C	33,32	33,19	33,44
Radiation temperature, °C	34,75	34,69	34,71
Total heat transfer rate, W	175,02	166,62	169,85

For the calculation of the PMV and PPV value the CBE Thermal Comfort Tool is used. That is web-based calculator developed by the Center for the Built Environment at UC Berkeley and is in compliance with a ASHRAE 55, ISO 7730 and EN 16798-1 standards.

Obtained PMV value is 0,83, while PPD is 20% according to EN 16798-1 standard.

The average temperatures on the passenger's body surface, obtained in the simulation, are in good agreement with the range considered physiologically neutral and comfortable for the human body in the literature (30-34°C) [9]. Given that the obtained average body surface temperatures in this simulation are within this recommended range, it can be concluded that the simulated ventilation conditions ensure a satisfactory thermal state of the passenger's body on average, although, as is shown at the Figure 5, local variations (especially in the head and lower extremities) may deviate from this neutral value.

The temperature distribution across the surfaces of the three occupants results reveal a clear vertical stratification of body-surface temperature, with the highest values at the head. This localized heating is consistent with the elevated temperatures identified on the interior roof surface, indicating that radiative heat transfer from the hot roof panel directly contributes to the thermal loading of the occupants head. In contrary, the back and upper torso region exhibits noticeably lower temperatures, in the range of approximately 29–35°C, which can be attributed to the direct impingement of the cold air jet discharged from the vents, as it can also be observed in the velocity contours from Figure 5. Moving further down the body, the lower torso and thigh region shows intermediate and elevated temperaturee, suggesting reduced local ventilation efficiency in this area and a corresponding accumulation of heat. Overall, this non-uniform thermal pattern across the body demonstrates that occupant thermal comfort cannot be adequately captured by a single average body temperature and supports the use of segment based approach in order to to properly characterize localized thermal sensation.

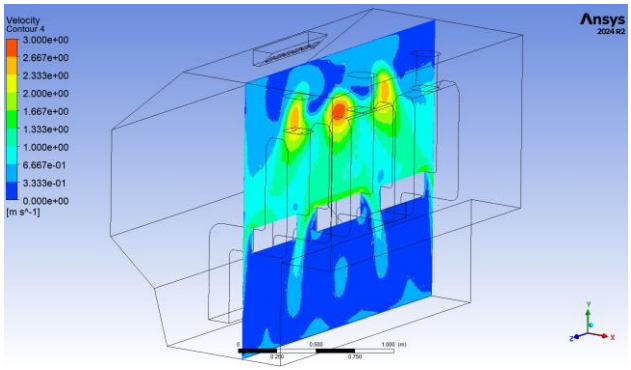


Figure 5. Velocity contours in the plane in front of the occupants

The temperature distribution on the interior surfaces of the cabin is shown in Figure 6. The results show pronounced spatial unevenness of the temperature field, with the highest values, up to 59.1°C, recorded on the windshield next to the cabin roof. These indicates that the windshield is the dominant source of radiant heat load inside the cabin, which is in line with physical expectations for a vehicle exposed to direct solar radiation. That suggests thermal insulation at the junction between the roof and the windshield, where thermal bridges are likely to be formed.

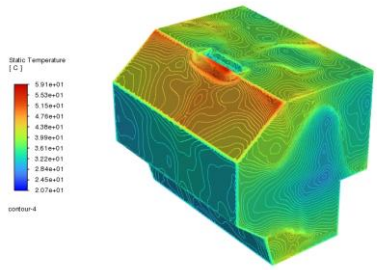


Figure 6. Temperature distribution on cabin interior surfaces (walls)

Considering the given conditions of speed angles, passengers can feel discomfort expressed in the form of uneven temperature on different parts of the body, primarily in the area of the legs and crown of the head. The applied heat flux has been increased on the safety side, so that in reality lower values are expected, and therefore less pronounced discomfort.

The distribution of air flow velocity in the longitudinal section of the cabin is shown by the vector field in Figure 7. The jet is directed downwards towards the central part of the cabin. After entering, the jet maintains a relatively high speed along a narrow vertical channel, after which it expands and gradually slows down due to mixing with the surrounding, much calmer air in the lower part of the cabin, where low flow speeds (below 2 m/s) dominate. This distribution is a direct consequence of the one-sided position of the inlet because entire airflow is supplied from one, upper side of the cabin, there is no symmetrical or multi-sided flow distribution along the longitudinal axis of the cabin, which leads to a pronounced velocity gradient between the central zone directly below the inlet and the front and rear of the cabin, where zones of lower velocity and potential stagnation are formed.

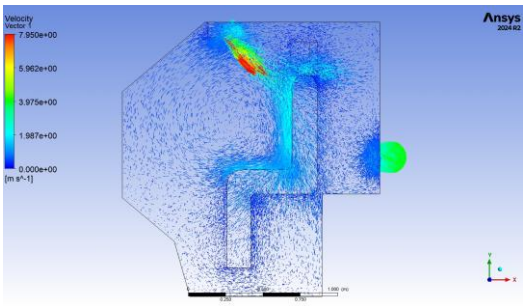


Figure 7. Velocity vector in cabin mid cross section

5. CONCLUSION

In this paper, a CFD analysis of thermal comfort and air flow in the cabin of a vehicle with three cabin crew members was carried out. The simulation included a cabin with a unique arrangement of air supply exclusively from the upper side of the cabin, which enabled a detailed analysis of the impact of spatially asymmetric configuration on the distribution of speed, temperature and thermal comfort indices of passengers.

The thermal comfort indices PMV and PPD calculated for the observed case were 0,83 and 20%, respectively, which is in good agreement with data obtained through experimental testing.

The results of this research indicate that the assessment of thermal comfort based solely on global, spatially averaged indices (PMV, PPD, average temperature) and simplified geometry does not fully include local variations of the thermal and velocity field inside the cabin, especially in the zones of direct interaction with air jets (head, chest) and solar heating zones (windshield and roof).

The obtained results contribute to a better understanding of airflow organization and heat transfer processes and provide a basis for future optimization of HVAC system performance, energy efficiency and occupant thermal comfort in special purpose vehicles.

References

[1] Brooks, M.-A. (2016). *Thermal modeling for light armored vehicle* [Master's thesis, University of Western Ontario]. https://ir.lib.uwo.ca/etd/3745

[2] BAESS labs solar irradiance calculator: https://www.baess.app/tools/solar-irradiance-calculator

[3] Fujita, A., Kanemaru, J., Nakagawa, H., & Ozeki, Y. (2001). Numerical simulation method to predict the thermal environment inside a car cabin. *JSAE Review*, 22(1), 39–47.

[4] Park et al. (2026). Comprehensive parametric study of cabin thermal comfort [proveri pun naslov]. *Applied Sciences*, 16(8), 3964. https://doi.org/10.3390/app16083964

[5] Pryor, R., Ditty, D., Mao, W., Rynes, P., & Smith, C. (2009). Development of a validated thermal model of AC performance in a protected combat ground vehicle. *Proceedings of GVSETS 2009*, NDIA/SAE, 1–7.

[6] Elasto Proxy. Military Vehicle Thermal Insulation. Technical reference (manufacturer data). https://www.elastoproxy.com/military-vehicle-thermal-insulation/

[7] Engineering ToolBox. Mineral Wool Insulation — Thermal Conductivity. Technical reference. https://www.engineeringtoolbox.com/mineral-wool-insulation-k-values-d_815.html

[8] https://www.ansys.com/

[9] Zhang, L., et al., Numerical Analysis of the Relationship Between Human Skin Temperature and Thermal Comfort. Proceedings of the ACM (2022). DOI: 10.1145/3501409.3501619